Transp Porous Med (2017) 118:495–518
DOI 10.1007/s11242-017-0867-3

Self-Consistent Channel Approach for Upscaling Chloride Diffusivity in Cement Pastes

Nattapong Damrongwiriyanupap[1,2] · **Stefan Scheiner**[1] · **Bernhard Pichler**[1] · **Christian Hellmich**[1]

Received: 22 April 2016 / Accepted: 25 April 2017 / Published online: 1 June 2017

Abstract Chloride ingress into concrete is a major cause for material degradation, such as cracking due to corrosion-induced steel reinforcement expansion. Corresponding transport processes encompass diffusion, convection, and migration, and their mathematical quantification as a function of the concrete composition remains an unrevealed enigma. Approaching the problem step by step, we here concentrate on the diffusivity of cement paste, and how it follows from the microstructural features of the material and from the chloride diffusivity in the capillary pore spaces. For this purpose, we employ advanced self-consistent homogenization theory as recently used for permeability upscaling, based on the resolution of the pore space as pore channels being oriented in all space directions, resulting in a quite compact analytical relation between porosity, pore diffusivity, and the overall diffusivity of the cement paste. This relation is supported by experiments and reconfirms the pivotal role that layered water most probably plays for the reduction of the pore diffusivity, with respect to the diffusivity found under the chemical condition of a bulk solution.

Keywords Diffusion · Homogenization · Chlorides · Multiscale modeling · Layered water

List of Symbols

Mathematical operators

div	Divergence operator, applied to a vector field
div	Divergence operator, applied to a second-order tensor field
grad	Gradient operator on the microscopic observation scale of pore space

✉ Stefan Scheiner
stefan.scheiner@tuwien.ac.at

1 Institute for Mechanics of Materials and Structures, TU Wien - Vienna University of Technology, Karlsplatz 13/202, 1040 Vienna, Austria

2 Civil Engineering Program, School of Engineering, University of Phayao, 19 Moo 2, Tumbol Maeka, Muang, Phayao 56000, Thailand

GRAD	Gradient operator on the macroscopic observation scale of cement paste
log	Natural logarithm
sin	Sine function
$\int f(x)\,\mathrm{d}x$	Integration of function f with respect to variable x
$\partial f/\partial x$	Partial differentiation of function f with respect to variable x
$\cdot$	First-order tensor contraction

Latin symbols

$\mathbf{A}_{\mathrm{pore}}$	Localization tensor for the concentration gradient of chloride ions in the pore space
c	Microscopic concentration of chloride ions
C	Macroscopic concentration of chloride ions
$\mathscr{D}$	Characteristic length of heterogeneities within a representative volume element
d_{bulk}	Chloride diffusion coefficient in bulk solution
d_{pore}	Chloride diffusion coefficient in the pore fluid, when considering isotropic pore diffusivity
$d_{\mathrm{pore}}^{\mathrm{long}}$	Longitudinal chloride diffusion coefficient in the pore fluid, when considering anisotropic pore diffusivity
$d_{\mathrm{pore}}^{\mathrm{trans}}$	Transverse chloride diffusion coefficient in the pore fluid, when considering anisotropic pore diffusivity
$\mathbf{d}_{\mathrm{pore}}$	Isotropic chloride diffusivity tensor in the pore fluid
$\mathbf{d}_{\mathrm{pore}}^{\mathrm{aniso}}$	Anisotropic chloride diffusivity tensor in the pore fluid
$\mathbf{d}_{\mathrm{solid}}$	Chloride diffusivity tensor in the solid phase
$D_{\mathrm{paste}}^{\mathrm{exp}}$	Experimentally obtained diffusion coefficient of chloride ions in cement paste
$D_{\mathrm{paste}}^{\mathrm{hom}}$	Homogenized diffusion coefficient of chloride ions in cement paste, when considering cylindrical pores with isotropic diffusivity
$D_{\mathrm{paste}}^{\mathrm{hom,sph}}$	Homogenized diffusion coefficient of chloride ions in cement paste, when considering spherical pores with isotropic diffusivity
$D_{\mathrm{paste}}^{\mathrm{hom,aniso}}$	Homogenized diffusion coefficient of chloride ions in cement paste, when considering cylindrical pores with anisotropic diffusivity
$\mathbf{D}_{\mathrm{paste}}^{\mathrm{hom}}$	Homogenized diffusivity tensor of chloride ions in cement paste, when considering cylindrical pores with isotropic diffusivity
$\mathbf{e}_x, \mathbf{e}_y, \mathbf{e}_z$	Unit base vectors of Cartesian coordinate system
$\mathbf{e}_r, \mathbf{e}_\vartheta, \mathbf{e}_\varphi$	Unit base vectors of spherical coordinate system
f_{air}	Volume fraction of air pores
f_{cem}	Volume fraction of cement clinker
f_{hyd}	Volume fraction of hydration products
f_{pore}	Volume fraction of pore space
f_{water}	Volume fraction of water
j	Index representing a specific data point
$\mathbf{j}$	Microscopic diffusive flux vector of chloride ions
$\mathbf{j}_{\mathrm{pore}}$	Microscopic diffusive flux vector of chloride ions in the pore space
$\mathbf{J}_{\mathrm{paste}}$	Macroscopic diffusive flux vector of chloride ions
l_{pore}	Length of single pore
ℓ	Characteristic length of representative volume element

$\mathscr{L}_\mathrm{C}$	Characteristic length of physical quantities related to a representative volume element
$\mathscr{L}_\mathrm{S}$	Characteristic length of a solid or structure made up by the material defined by a representative volume element
n	Number of experimental data points
$\mathbf{P}_\mathrm{pore}$	Hill tensor related to the pore space
$\mathbf{P}_\mathrm{solid}$	Hill tensor related to the solid phase
r	Radial coordinate of spherical coordinate system
R^2	Coefficient of determination
RVE	Representative volume element
s	Standard deviation of the $(d_{\mathrm{pore},i}/d^*_{\mathrm{pore},i})$-population
$t_{n-1,\alpha/2}$	t-value
V_RVE	Volume of representative volume element
∂V_RVE	Surface of representative volume element
w/c	Initial water-to-cement mass ratio
$(w/c)_\mathrm{cur}$	Water-to-cement mass ratio after curing
$\mathbf{x}$	Position vector
$\bar{x}$	Mean value of the $(d_{\mathrm{pore},i}/d^*_{\mathrm{pore},i})$-population
$z_{\alpha/2}$	z-value
$\mathbf{1}$	Second-order unit tensor

Greek letters

α	Statistical significance level
ϑ	Euler angle
ξ	Degree of cement hydration
μ	Expected value
μ_low	Lower bound of the expected value
μ_up	Upper bound of the expected value
σ_up	Upper bound for the standard deviation
φ	Euler angle
$\chi^2_{n-1,\alpha}$	χ^2-value

1 Introduction

Ingress of chloride ions into steel-reinforced concrete structures is an important factor for initiating corrosion of the embedded steel bars (Glass and Buenfeld 1997). The presence of chloride ions in concrete structures is thus considered a major threat to their durability (Stewart and Rosowsky 1998). The underlying transport processes comprise diffusion, migration, and convection (Glasser et al. 2008), and their interplay turns out as complex, so that studying these processes individually is generally considered as a suitable scientific approach. In this context, the chloride diffusivity of concrete in particular, and of cementitious materials in general, is a (so far only partially resolved) topic of great scientific interest. Here, the key challenge lies in the fact that this diffusivity is not constant, but depends on the composition of the material (governed by the chosen mixture, standardly expressed in terms of the initial water-to-cement mass ratio and the initial aggregate-to-cement mass ratio), of its maturity (quantified by the so-called degree of hydration), as well as of microcracks occurring at the interfaces between aggregate grains (referred to as "bond cracks") or connecting different

aggregate grains (referred to as "matrix cracks"), as shown in (Wong et al. 2009; Wu et al. 2015).

Striving for understanding this composition dependence, numerous experimental campaigns provided valuable insights, and the latter were often condensed into (more or less appropriate) simplified empirical relations (Page and Ngala 1997; Oh and Jang 2004; Sun et al. 2011b). Importantly, the majority of such diffusion tests have been carried out on cement paste specimens (concrete is regarded as composite consisting of cement paste and aggregates—in the present paper, we focus on the chloride diffusivity of cement paste as well. This focus on cement paste implies that the aforementioned microcracks, potentially exerting a substantial influence on the macroscopic diffusivity of mortar or concrete, can be neglected subsequently.

From a more fundamental viewpoint, it is natural to explore the microstructural sources which drive the overall diffusive properties of cement paste, and to derive corresponding mathematical functions taking into account the relevant information available at the microlevel. In this context, repeated inclusion of infinitely small solid spheres into a repeatedly homogenized diffusive medium, as is customarily done in the so-called differential schemes (Dormieux and Lemarchand 2001), proposes that the isotropic diffusivity of cement paste depends on the (capillary) fluid volume fraction to the power of 1.5, times the chloride diffusivity of the pore solution. This allows for translating experimental data obtained from cement paste specimens with different mixtures into one "universal" chloride diffusivity of the cement paste pore solution, $d_{\text{pore}} = 1.07 \times 10^{-10}\,\text{m}^2/\text{s}$ (Pivonka et al. 2004). Interestingly, this value for d_{pore} is about 15 times smaller than the chloride diffusivity of a bulk solution, $d_{\text{bulk}} = 1.61 \times 10^{-9}\,\text{m}^2/\text{s}$ (Robinson and Stokes 1959). This is probably due to the charged pore surfaces causing water structuring, which, in turn, leads to a reduction of the solution's diffusivity. The aforementioned diffusivity difference in bulk versus electrically influenced solutions was subsequently confirmed by additional studies (Zheng and Zhou 2008; Zheng et al. 2009a, 2010; Liu et al. 2012), and the aforementioned chloride diffusivity of the cement paste solution turned out to be an appropriate input for various simulations dealing with the durability of concrete, see, e.g., (Liu et al. 2013; Du et al. 2014). Alternatively, still considering spherical morphological features, concrete diffusivity upscaling was achieved by means of the so-called Maxwell effective medium approach, for studying the effects of entrapped air pores (Wong et al. 2011) and interphases (Lutz and Zimmerman 2015) on the macroscopic diffusivity.

However, cement paste actually exhibits clearly non-spherical microstructural features. Explicit consideration of the latter has allowed for substantial improvements of microstructural models for the *mechanics* of cement paste and concrete (Sanahuja et al. 2007; Pichler et al. 2009a; Pichler and Hellmich 2011). The same is true for a micromechanical model of gypsum which considers the physically active (solid) parts of the microstructure as infinitely many non-spherical phases (Sanahuja et al. 2010), while the physically non-active (fluid) parts were considered, for simplicity, as spheres. This gypsum model was shown to predict homogenized elastic properties as precisely as corresponding full 3D Finite Element simulations (Meille and Garboczi 2001). Thus, the question arises whether the upscaling-based estimate of the chloride diffusivity of the cement paste pore solution can be as well improved when considering a more realistic microstructural representation of cement paste. This motivates us to adapt, in the present paper, the aforementioned homogenization approach based on infinitely many non-spherical phases, for diffusivity upscaling. In particular, we address (i) whether such a more sophisticated and physically profound approach would replicate the experimental data in a more suitable way than the classical differential method-based approach, and (ii) whether and how the corresponding estimate of the chloride diffusiv-

ity in the cement paste pore solution changes with respect to its differential method-based counterpart.

For this purpose, we first present the model representation of cement paste, considering the concepts of scale separation and random homogenization (see Sect. 2). Then, a new self-consistent homogenization scheme for estimating the chloride diffusivity in cement paste is derived (see Sect. 3), and the chloride diffusivity in the cement paste pore solution is assessed (see Sect. 4). After a comprehensive discussion (see Sect. 5), a brief summary and outlook concludes the paper (see Sect. 6).

2 Representative Volume Element for Diffusive Transport in Cement Paste

We here introduce a representative volume element (RVE) fulfilling the standard "separation of scales"-requirement needed for random homogenization methods or continuum micromechanics (Zaoui 2002; Drugan and Willis 1996; Dormieux and Kondo 2005). Inside the RVE, microscopic ionic fluxes $\mathbf{j}$ fulfill the mass conservation law (Dormieux and Lemarchand 2001)

$$\forall \mathbf{x} \in V_{\mathrm{RVE}} : \ \operatorname{div} \mathbf{j}(\mathbf{x}) = 0, \tag{1}$$

with the position vector $\mathbf{x}$ labeling points within the RVE and at its boundary. Equation (1) can be transformed into the so-called weak form, analogous to the principle of virtual power in mechanics, see, e.g., (Germain 1973; Kuhl et al. 2004; Zienkiewicz et al. 2005; Maugin 2013), through multiplication with an arbitrary test function $c(\mathbf{x})$, and integration over the domain of the RVE, yielding

$$\begin{aligned} \int_{V_{\mathrm{RVE}}} c(\mathbf{x})[\operatorname{div} \mathbf{j}(\mathbf{x})]\, \mathrm{d}V &= \int_{V_{\mathrm{RVE}}} \mathbf{j}(\mathbf{x}) \cdot \mathbf{grad}\, c(\mathbf{x})\, \mathrm{d}V \\ &= \int_{V_{\mathrm{RVE}}} \operatorname{div} [\mathbf{j}(\mathbf{x}) c(\mathbf{x})]\, \mathrm{d}V \\ &= \int_{\partial V_{\mathrm{RVE}}} [\mathbf{j}(\mathbf{x}) c(\mathbf{x}) \cdot \mathbf{n}(\mathbf{x})]\, \mathrm{d}S, \end{aligned} \tag{2}$$

whereby use of Eq. (1) was made, and with $\partial V_{\mathrm{RVE}}$ denoting the boundary of the RVE. It is suitable to assign, to the test function, the nature of a "virtual concentration"; namely when defining boundary conditions for the RVE. Following (Dormieux and Lemarchand 2001), we prescribe "microscopic" concentrations at the boundary of the RVE of cement paste, which are compatible with a homogeneous "macroscopic" concentration gradient $\mathbf{GRAD}\, C$; this reads mathematically as

$$\forall \mathbf{x} \in \partial V_{\mathrm{RVE}} : c(\mathbf{x}) = \mathbf{GRAD}\, C \cdot \mathbf{x}. \tag{3}$$

Using Eq. (3) in Eq. (2) yields

$$\begin{aligned}\int_{V_{\mathrm{RVE}}} \mathbf{j}(\mathbf{x}) \cdot \mathbf{grad}\, c(\mathbf{x})\, \mathrm{d}V &= \int_{\partial V_{\mathrm{RVE}}} [\mathbf{j}(\mathbf{x}) c(\mathbf{x}) \cdot \mathbf{n}(\mathbf{x})]\, \mathrm{d}S \\ &= \int_{\partial V_{\mathrm{RVE}}} (\mathbf{GRAD}\, C \cdot \mathbf{x})[\mathbf{j}(\mathbf{x}) \cdot \mathbf{n}(\mathbf{x})]\, \mathrm{d}S \\ &= \mathbf{GRAD}\, C \cdot \int_{\partial V_{\mathrm{RVE}}} [\mathbf{x} \otimes \mathbf{j}(\mathbf{x})] \cdot \mathbf{n}(\mathbf{x})\, \mathrm{d}S \\ &= \mathbf{GRAD}\, C \cdot \int_{V_{\mathrm{RVE}}} \mathbf{div}\, [\mathbf{x} \otimes \mathbf{j}(\mathbf{x})]\, \mathrm{d}V \\ &= \mathbf{GRAD}\, C \cdot \int_{V_{\mathrm{RVE}}} \mathbf{j}(\mathbf{x})\, \mathrm{d}V.\end{aligned} \tag{4}$$

Equation (4) readily suggests to introduce a macroscopic ionic flux $\mathbf{J}_{\mathrm{paste}}$ in the format

$$\int_{V_{\mathrm{RVE}}} \mathbf{j}(\mathbf{x}) \cdot \mathbf{grad}\, c(\mathbf{x})\, \mathrm{d}V = V_{\mathrm{RVE}} \mathbf{J}_{\mathrm{paste}} \cdot \mathbf{GRAD}\, C, \tag{5}$$

which implies the following average rule for the ionic fluxes:

$$\mathbf{J}_{\mathrm{paste}} = \frac{1}{V_{\mathrm{RVE}}} \int_{V_{\mathrm{RVE}}} \mathbf{j}(\mathbf{x})\, \mathrm{d}V. \tag{6}$$

As the microstructure within the RVE is, as a rule, never known in minute detail, it is represented in the simplest possible (while still sufficiently complex) way, by means of homogeneous subdomains within the RVE, called "material phases." In the present case, these phases are characterized by quantitative properties, namely volume fractions and (chloride) diffusivities: One (spherical) solid phase with volume fraction $(1 - f_{\mathrm{pore}})$ exhibits negligible diffusivity ($\mathbf{d}_{\mathrm{solid}} \approx 0$), while infinitely many, arbitrarily oriented (elongated) cylindrical pore phases fill the remaining volume (with volume fraction f_{pore}) and exhibit the (chloride) diffusivity of the pore fluid, $\mathbf{d}_{\mathrm{pore}}$, see Fig. 1. Specification of Eq. (6) for this morphology yields

$$\mathbf{J}_{\mathrm{paste}} = f_{\mathrm{pore}} \int_{\varphi=0}^{2\pi} \int_{\vartheta=0}^{\pi} \mathbf{j}_{\mathrm{pore}}(\vartheta, \varphi) \frac{\sin \vartheta}{4\pi} \mathrm{d}\vartheta\, \mathrm{d}\varphi, \tag{7}$$

with $\mathbf{j}_{\mathrm{pore}}(\vartheta, \varphi)$ denoting the ionic flow characterizing the cylindrical pore phase oriented in (ϑ, φ)-direction according to Fig. 2. Notably, Eq. (7) considers that no fluxes occur in the solid phase, see also (Dormieux and Lemarchand 2001). Transport in the pores is governed by Fick's first law of diffusion, reading in a phase-specific format as

$$\mathbf{j}_{\mathrm{pore}}(\vartheta, \varphi) = -\mathbf{d}_{\mathrm{pore}}(\vartheta, \varphi) \cdot (\mathbf{grad}\, c)_{\mathrm{pore}}(\vartheta, \varphi), \tag{8}$$

whereby the phase-specific diffusivity tensor always exhibits the same eigenvalues, and eigendirections which are aligned with the pore directions. This tensor relates the orientation-specific ionic flux to the concentration gradient by which it is driven, i.e., to the orientation-specific concentration gradient $(\mathbf{grad}\, c)_{\mathrm{pore}}(\vartheta, \varphi)$.

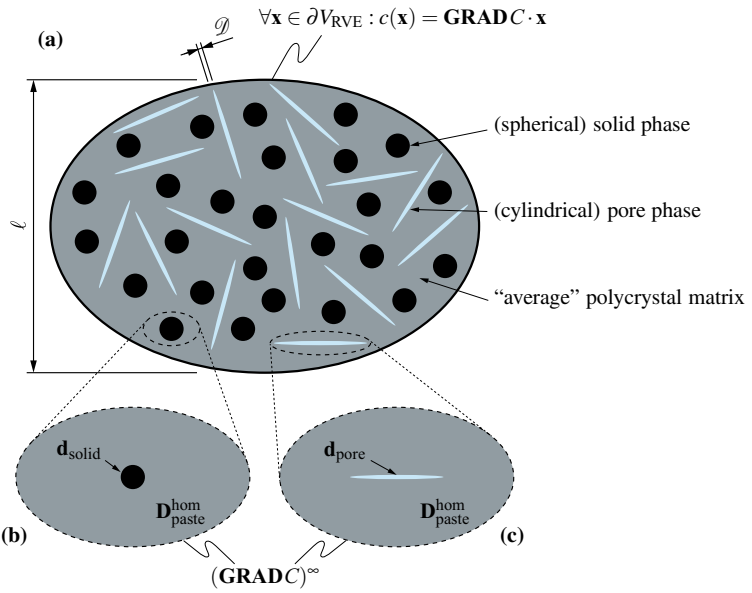

Fig. 1 2D illustration of the *3D micromechanical representation of cement paste*: **a** polycrystal-type arrangement of (*spherical*) solid and (*cylindrical*) pore phases, with indication of the characteristic lengths of heterogeneities, $\mathscr{D}$, and of the RVE, ℓ, $\mathscr{D} \ll \ell$, whereas ℓ is significantly smaller than the characteristic lengths of physical quantities related to the RVE, $\mathscr{L}_{\mathrm{C}}$, and of a solid or structure made up by the material defined by the RVE, $\mathscr{L}_{\mathrm{S}}$, $\ell \ll \{\mathscr{L}_{\mathrm{C}}, \mathscr{L}_{\mathrm{S}}\}$; **b** and **c** show the matrix-inclusion problems used for the derivation of localization tensor $\mathbf{A}_{\mathrm{pore}}$, see Sect. 3

3 Homogenization of Macroscopic Diffusion Behavior: Porosity–Diffusivity Relations

Due to the linearities of both the considered transport law and the mass conservation law, a linear macro-to-micro "downscaling" relation can be established for the concentration gradients,

$$(\mathbf{grad}\, c)_{\mathrm{pore}}(\vartheta, \varphi) = \mathbf{A}_{\mathrm{pore}}(\vartheta, \varphi) \cdot \mathbf{GRAD}\, C, \tag{9}$$

with $\mathbf{A}_{\mathrm{pore}}$ as the second-order "downscaling" or localization tensor (alternatively also referred to as concentration tensor) related to the concentration gradient of chloride ions encountered in the pore space; such localization tensors have been originally defined for linear elasticity (Zaoui 1997, 2002), and later also for pressure gradients driving Darcy-type fluid flow (Dormieux and Kondo 2004, 2005). Derivation of $\mathbf{A}_{\mathrm{pore}}$ has been dealt with in great detail in (Abdalrahman et al. 2015), based on Eshelby's famous inhomogeneity problem (Eshelby 1957), see also the work of Dormieux and Kondo (2005), eventually yielding

$$\begin{aligned}\mathbf{A}_{\mathrm{pore}}(\vartheta, \varphi) = &\left[\mathbf{1} + \mathbf{P}_{\mathrm{pore}}(\vartheta, \varphi) \cdot \left(\mathbf{d}_{\mathrm{pore}} - D^{\mathrm{hom}}_{\mathrm{paste}}\mathbf{1}\right)\right]^{-1} \cdot \Big\{(1 - f_{\mathrm{pore}})\left[\mathbf{1} - \mathbf{P}_{\mathrm{solid}} \cdot D^{\mathrm{hom}}_{\mathrm{paste}}\mathbf{1}\right]^{-1} \\ &+ f_{\mathrm{pore}} \int_{\varphi=0}^{2\pi} \int_{\vartheta=0}^{\pi} \left[\mathbf{1} + \mathbf{P}_{\mathrm{pore}}(\vartheta, \varphi) \cdot \left(\mathbf{d}_{\mathrm{pore}} - D^{\mathrm{hom}}_{\mathrm{paste}}\mathbf{1}\right)\right]^{-1} \frac{\sin\vartheta}{4\pi} \mathrm{d}\vartheta\, \mathrm{d}\varphi \Big\}^{-1},\end{aligned} \tag{10}$$

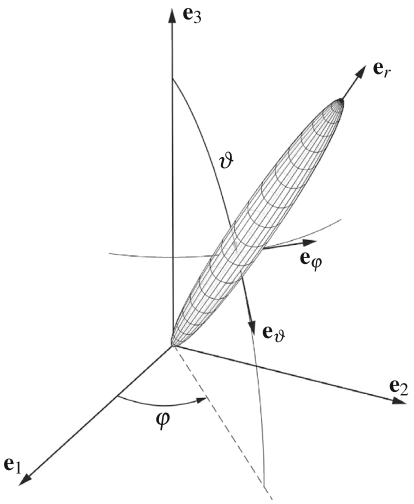

Fig. 2 *Cylindrical pore space inclusion* oriented along vector $\mathbf{e}_r$, and inclined by the Euler angles ϑ and φ, with respect to the reference base frame defined through the unit vectors $\mathbf{e}_1$, $\mathbf{e}_2$, and $\mathbf{e}_3$; the local base frame, defined by unit vectors $\mathbf{e}_r$, $\mathbf{e}_\vartheta$, and $\mathbf{e}_\varphi$, is attached to the cylindrical inclusion

where $D^{\text{hom}}_{\text{paste}}$ is the homogenized macroscopic diffusion coefficient of chloride ions in cement paste. Furthermore, $\mathbf{P}_{\text{pore}}$ and $\mathbf{P}_{\text{solid}}$, respectively, denote the so-called Hill or morphology tensors accounting for the shape of an ellipsoidal inhomogeneity of diffusivities $\mathbf{d}_{\text{pore}}$ and $\mathbf{d}_{\text{solid}} = d_{\text{solid}}\mathbf{1}$, respectively, embedded in a fictitious matrix with diffusivity $\mathbf{D}^{\text{hom}}_{\text{paste}} = D^{\text{hom}}_{\text{paste}}\mathbf{1}$. Given the micromechanical representation chosen for cement paste, see Sect. 2, the Hill tensors follow as (Dormieux et al. 2006; Abdalrahman et al. 2015)

$$\mathbf{P}_{\text{pore}}(\vartheta,\varphi) = \frac{1}{2D^{\text{hom}}_{\text{paste}}} \begin{bmatrix} 0 & 0 & 0 \\ 0 & 1 & 0 \\ 0 & 0 & 1 \end{bmatrix}_{\mathbf{e}_r,\mathbf{e}_\vartheta,\mathbf{e}_\varphi}, \tag{11}$$

representing a cylindrical shape with its orientation defined through angles ϑ and φ, and

$$\mathbf{P}_{\text{solid}} = \frac{1}{3D^{\text{hom}}_{\text{paste}}} \begin{bmatrix} 1 & 0 & 0 \\ 0 & 1 & 0 \\ 0 & 0 & 1 \end{bmatrix}, \tag{12}$$

representing a spherical shape. The tensor components of $\mathbf{P}_{\text{pore}}$ need to be transformed from the $(\mathbf{e}_r, \mathbf{e}_\varphi, \mathbf{e}_\varphi)$-base to the $(\mathbf{e}_1, \mathbf{e}_2, \mathbf{e}_3)$-base, through the standard transformation laws for second-order tensors (Salençon 2001). $\mathbf{P}_{\text{solid}}$, in turn, is an isotropic tensor, and its components remain unchanged upon any component transformation.

Using Eq. (9) in Eq. (7) yields

$$\mathbf{J}_{\text{paste}} = -\left\{ f_{\text{pore}} \int_{\varphi=0}^{2\pi} \int_{\vartheta=0}^{\pi} \mathbf{d}_{\text{pore}}(\vartheta,\varphi) \cdot \mathbf{A}_{\text{pore}}(\vartheta,\varphi) \frac{\sin\vartheta}{4\pi} \mathrm{d}\vartheta\, \mathrm{d}\varphi \right\} \cdot \mathbf{GRAD}\, C. \tag{13}$$

Inserting the macroscopic ionic flux according to Eq. (13) into Fick's first law at the macroscopic observation scale,

$$\mathbf{J}_{\text{paste}} = -\mathbf{D}^{\text{hom}}_{\text{paste}} \cdot \mathbf{GRAD}\, C, \tag{14}$$

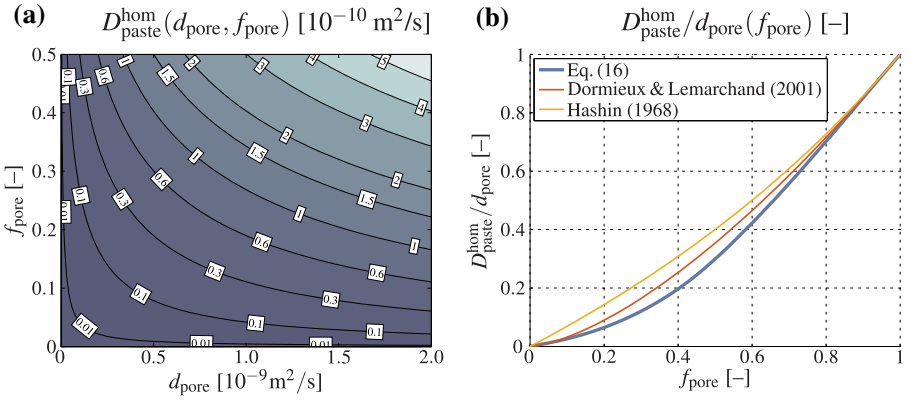

Fig. 3 Parametric study showing **a** how the macroscopic chloride diffusion coefficient $D^{\mathrm{hom}}_{\mathrm{paste}}$ is governed by the cement paste porosity f_{pore}, and the microscopic (pore-scale) chloride diffusion coefficient d_{pore}, based on evaluation of Eq. (16); and **b** the porosity-dependent ratio of $D^{\mathrm{hom}}_{\mathrm{paste}}$ to d_{pore}, comparing the self-consistent homogenization scheme resulting in Eq. (16), on the differential homogenization scheme by Dormieux and Lemarchand (2001), and on the self-consistent bispherical model of Hashin (1968)

gives, by comparing Eqs. (13) and (14), finally access to the macroscopic diffusivity tensor $D^{\mathrm{hom}}_{\mathrm{paste}}$:

$$\mathbf{D}^{\mathrm{hom}}_{\mathrm{paste}} = f_{\mathrm{pore}} \int_{\varphi=0}^{2\pi} \int_{\vartheta=0}^{\pi} \mathbf{d}_{\mathrm{pore}}(\vartheta, \varphi) \cdot \mathbf{A}_{\mathrm{pore}}(\vartheta, \varphi) \frac{\sin\vartheta}{4\pi} \mathrm{d}\vartheta \, \mathrm{d}\varphi = D^{\mathrm{hom}}_{\mathrm{paste}} \mathbf{1}. \tag{15}$$

For simplicity, we now choose to assume isotropic chloride diffusivity in the pore space, thus $\mathbf{d}_{\mathrm{pore}}(\vartheta, \varphi) = d_{\mathrm{pore}}\mathbf{1}$. Then, insertion of Eqs. (11) and (12) into Eq. (10), and insertion of the corresponding result into Eq. (15), allows us to derive a quadratic equation that can be straightforwardly solved for $D^{\mathrm{hom}}_{\mathrm{paste}}$:

$$D^{\mathrm{hom}}_{\mathrm{paste}} = \frac{d_{\mathrm{pore}}}{2(f_{\mathrm{pore}}+9)} \left[3\left(33 f_{\mathrm{pore}}^2 - 26 f_{\mathrm{pore}} + 9\right)^{0.5} + 17 f_{\mathrm{pore}} - 9 \right]. \tag{16}$$

The micro–macro relation given by Eq. (16) reveals the homogenized diffusivity of cement paste as a function of pore diffusivity and porosity, $D^{\mathrm{hom}}_{\mathrm{paste}} = F(f_{\mathrm{pore}}, d_{\mathrm{pore}})$, see Fig. 3(a). Dividing both sides of Eq. (16) by d_{pore} readily yields a dimensionless format of this micro–macro relation, reading as $D^{\mathrm{hom}}_{\mathrm{paste}}/d_{\mathrm{pore}} = \mathscr{F}(f_{\mathrm{pore}})$, see Fig. 3(b). Comparing the latter ratio to the classical results of Dormieux and Lemarchand (2001), who considered a differential homogenization scheme, yielding $D^{\mathrm{hom}}_{\mathrm{paste}}/d_{\mathrm{pore}} = f^{1.5}_{\mathrm{pore}}$, and of Hashin (1968), who considered a self-consistent homogenization scheme based on a bispherical morphology, yielding $D^{\mathrm{hom}}_{\mathrm{paste}}/d_{\mathrm{pore}} = 2f_{\mathrm{pore}}/(3 - f_{\mathrm{pore}})$ shows that due to the revised morphology, our model leads to significantly lower homogenized cement paste diffusivities at low porosities.

4 Upscaling Theory-Guided Re-evaluation of Diffusion Experiments: Access to Chloride Diffusivity at the Capillary Pore Level

As direct experimental determination of d_{pore} is out of reach (due to the small pore scales, in comparison with standard diffusivity testing devices), we will check whether many different

diffusivity tests at the level of cement paste, with different porosities f_{pore}, deliver, via Eq. (16), the same (or at least) similar values for the pore diffusivity. Such diffusivity tests are, as a rule, not directly characterized by the porosity f_{pore}, but rather given in term of the initial water-to-cement mass ratio (w/c), at which the cement paste was produced, see Table 1. According to the famous Powers–Acker model (Powers and Brownyard 1948; Acker 2001), the water-to-cement ratio relates to the volume fractions of cement paste constituents "cement clinker" (cem), "water," "hydrates" (hyd), and "air," via (Pichler et al. 2009a)

$$f_{\text{cem}}(\xi) = \frac{20(1-\xi)}{20+63(w/c)} \geq 0, \tag{17}$$

$$f_{\text{water}}(\xi) = \frac{63\,[(w/c)-0.42\xi]}{20+63(w/c)} \geq 0, \tag{18}$$

$$f_{\text{hyd}}(\xi) = \frac{43.15\xi}{20+63(w/c)}, \tag{19}$$

$$f_{\text{air}}(\xi) = \frac{3.31\xi}{20+63(w/c)}, \tag{20}$$

with $f_{\text{cem}}(\xi)+f_{\text{water}}(\xi)+f_{\text{hyd}}(\xi)+f_{\text{air}}(\xi) = 1$ within an RVE of cement paste. In Eqs. (17)–(20), ξ denotes the degree of hydration, f_{cem} the volume fraction of unhydrated cement, f_{water} the volume fraction of water, f_{hyd} the volume fraction of hydrates, and f_{air} the volume fraction of air pores. Note that in the presently chosen model representation of cement paste, see Fig. 1, no distinction is made between hydrates and unhydrated cement grains; instead, both are considered as non-diffusible, and thus "merged" to one solid phase. Furthermore, since the considered experimental works, see Table 1, exclusively comprise classical diffusion or migration cell tests, in the course of which the cement paste sample is tested after the relevant pore spaces became water-saturated, also no distinction is required between water and air phase; they can be merged to one pore phase. As regards the cement paste mixture, an initial water-to-cement mass ratio smaller than 0.42 usually leads to incomplete hydration of cement paste; thus, a certain portion of unhydrated cement remains. However, all pastes considered here were cured in water for time periods of at least 4 weeks, which implies sufficient additional water supply beyond that accounted for in the initial water-to-cement ratio, so that eventually the entire cement clinker became hydrated (Pivonka et al. 2004). In order to consider this situation when computing the pore space volume fractions, we follow the strategy proposed by Pivonka et al. (2004) and introduce the water-to-cement mass ratio after curing, $(w/c)_{\text{cur}}$, being identical to the initial water-to-cement mass ratio for $(w/c) \geq 0.42$, and amounting to 0.42 for pastes with $(w/c) < 0.42$. In addition, the aforementioned curing times also propose consideration of completed hydration, $\xi = 1$. Then, the volume fraction of the chloride diffusion-enabling pore space reads as

$$f_{\text{pore}}(\xi=1) = f_{\text{water}}(\xi=1) + f_{\text{air}}(\xi=1) = \frac{29.77+63(w/c)_{\text{cur}}}{20+63(w/c)_{\text{cur}}}, \tag{21}$$

see the fifth column of Table 1.

Equation (16) allows us to find, for each data pair f_{pore} and $D^{\text{exp}}_{\text{paste}}$, one corresponding value for d_{pore}, see the last column of Table 1. Such obtained pore diffusivity values are indeed well clustered around their mean value $\bar{d}_{\text{pore}} = 1.476 \times 10^{-10}\,\text{m}^2/\text{s}$, with a standard deviation of $5.049 \times 10^{-11}\,\text{m}^2/\text{s}$.

It is also interesting to check the statistical relevance of the identified mean pore diffusivity value in combination with the upscaling model of Sect. 3, in comparison with the porosity–diffusivity relations given through the experimental values documented in Table 1,

Table 1 Experimentally determined chloride diffusion coefficients in cement paste ($D^{\text{exp}}_{\text{paste}}$); the corresponding pore space volume fractions (f_{pore}) follow from cement paste mixture rules, see (Pivonka et al. 2004; Acker 2001) for details; pore-scale diffusivity d_{pore} follows from evaluation of Eq. (16), for the respective data pairs (f_{pore}; $D^{\text{exp}}_{\text{paste}}$)

References	Short name	w/c [−]	$(w/c)_{\text{cur}}$ [−]	f_{pore} [−]	$D^{\text{exp}}_{\text{paste}}$ [10^{-12} m^2/s]	d_{pore} [10^{-10} m^2/s]
Page et al. (1981)	P81	0.40	0.42	0.071	2.600	1.451
		0.50	0.50	0.162	4.470	0.922
		0.60	0.60	0.254	12.350	1.349
Yu and Page (1991)	Y91	0.35	0.42	0.071	1.200	0.670
		0.50	0.50	0.162	5.430	1.120
		0.60	0.60	0.254	7.300	0.798
Tang and Nilson (1992)	T92	0.40	0.42	0.071	2.900	1.162
		0.60	0.60	0.254	9.400	1.027
		0.80	0.80	0.387	21.000	1.130
Hornain et al. (1995)	H95	0.55	0.55	0.210	11.250	1.621
MacDonald and Northwood (1995)	M95	0.40	0.42	0.071	2.353	1.313
		0.40	0.42	0.071	2.549	1.422
		0.40	0.42	0.071	2.784	1.554
		0.50	0.50	0.162	6.412	1.322
		0.50	0.50	0.162	6.745	1.391
		0.50	0.50	0.162	7.275	1.500
		0.60	0.60	0.254	12.290	1.343
		0.60	0.60	0.254	12.570	1.373
		0.60	0.60	0.254	13.840	1.512
		0.70	0.70	0.327	18.730	1.356
		0.70	0.70	0.327	21.570	1.562
		0.70	0.70	0.327	21.860	1.583

Table 1 continued

References	Short name	w/c [−]	$(w/c)_{cur}$ [−]	f_{pore} [−]	D^{exp}_{paste} [10^{-12} m^2/s]	d_{pore} [10^{-10} m^2/s]
Ngala et al. (1995)	N95	0.40	0.42	0.071	3.950	2.204
		0.50	0.50	0.162	7.800	1.609
		0.60	0.60	0.254	12.600	1.377
		0.70	0.70	0.327	21.460	1.554
Ngala and Page (1997)	N97	0.40	0.42	0.071	4.280	2.388
		0.50	0.50	0.162	8.430	1.739
		0.60	0.60	0.254	12.300	1.344
		0.70	0.70	0.327	21.380	1.548
Castellote et al. (2001)	C01	0.40	0.42	0.071	3.646	2.035
Caré (2003)	C03	0.45	0.45	0.108	5.650	1.953
Huang et al. (2010)	H10	0.40	0.42	0.071	5.420	3.025
		0.50	0.50	0.162	8.240	1.700
		0.60	0.60	0.254	12.000	1.311
Sun et al. (2011a)	S11	0.23	0.42	0.071	1.030	0.575
		0.35	0.42	0.071	4.120	2.299
		0.53	0.53	0.192	10.600	1.741

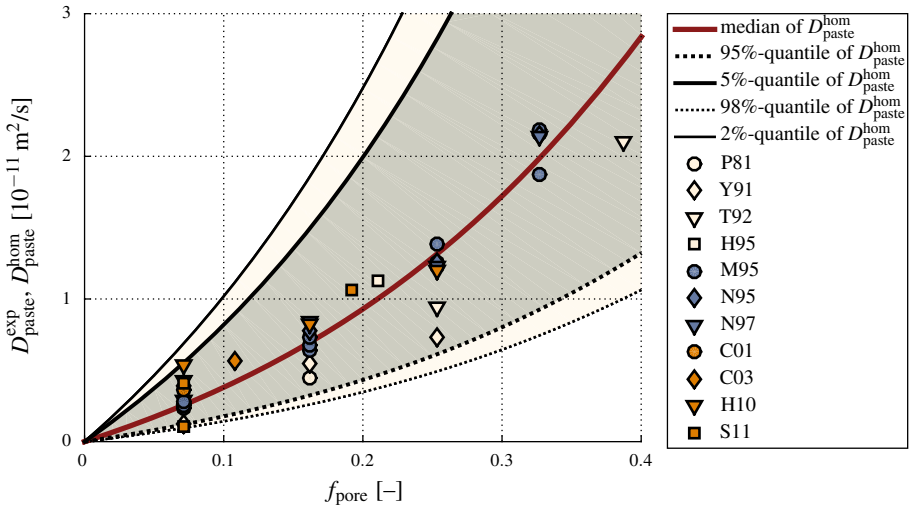

Fig. 4 Comparison of model-predicted and experimentally determined chloride diffusion coefficients in cement paste: experimental data, see Table 1, versus model predictions provided by Eq. (16), considering the pore diffusivities given in Eqs. (28) and (29) as well as the porosities listed in Table 1

as illustrated by different (triangle-, square-, and diamond-shaped) symbols in Fig. 4. For this purpose, we derive, from the statistical sample of pore diffusivities of Table 1, a complete statistical population of such values, and then take the 5 and 95% quantiles of this population for estimating upper and lower bounds for paste-related porosity–diffusivity relations. In more detail, we adapt the procedure proposed by König et al. (1998) in the context of the compressive strength of concrete, and refined by Pichler et al. (2005) for the impact of rock boulders onto gravel: Considering that the chloride diffusivities can take only positive values, the log-normal distribution appears as particularly relevant to capture the type of scattering observed with d_{pore}. That implies that the logarithms of the macroscopic diffusion coefficients, back-computed by means of Eq. (16) from whatever experimental realization of a diffusion test on cement paste, make up a normally distributed statistical population. Through taking the logarithms of the values given in Table 1, we obtain one statistical sample of the aforementioned statistical population. The elements of this sample are denoted as $\log(d_{\mathrm{pore},i}/d^*_{\mathrm{pore},i})$, where i is an index, $d_{\mathrm{pore},i}$ is the ith back-analyzed pore-scale diffusion coefficient, and d^*_{pore} is a normalization quantity, $d^*_{\mathrm{pore}} = 1\,\mathrm{m}^2/\mathrm{s}$, included to yield dimensionless arguments for the logarithmic function. The sample is characterized by a mean value $\bar{x}$ and standard deviation s, according to

$$\bar{x} = \frac{1}{n}\sum_{i=1}^{n} \log\left(\frac{d_{\mathrm{pore},i}}{d^*_{\mathrm{pore},i}}\right) = -22.663, \tag{22}$$

and

$$s = \sqrt{\frac{1}{n-1}\sum_{i=1}^{n}\left[\log\left(\frac{d_{\mathrm{pore},i}}{d^*_{\mathrm{pore},i}}\right) - \bar{x}\right]^2} = 0.323, \tag{23}$$

where $n = 38$ is the number of back-analyzed pore-scale diffusion coefficients. According to a famous result published by William Sealy Gosset alias "Student" (Student 1908), the

normalized differences between the mean values of any sample taken from a statistical population and the mean of the population itself follow a Student t-distribution of degree $(n-1)$, see, e.g., (Bortz 1999). This allows one to estimate upper and lower bounds of the statistical populations from the one known mean value of one sample taken from the population, according to

$$\mu_{\text{low}} = \bar{x} - \frac{(t_{n-1,1-\alpha/2})s}{\sqrt{n}} \leq \mu \leq \mu_{\text{up}} = \bar{x} + \frac{(t_{n-1,1-\alpha/2})s}{\sqrt{n}}, \tag{24}$$

where $t_{n-1,1-\alpha/2}$ is the so-called t-value, cutting an area equal to $1-\alpha/2$ of the Student's t-distribution with $n-1$ degrees of freedom, and α is the significance level, i.e., corresponding to $(1-\alpha)$-confidence interval. Considering the sample size $n = 38$ and the significance level $\alpha = 5\%$, one obtains $t_{n-1,1-\alpha/2} = 2.026$. Then, Eq. (24) allows us to calculate $\mu_{\text{low}} = -22.767$ and $\mu_{\text{low}} = -22.556$. The upper bound of the respective standard deviation σ, σ_{up}, is based on a one-sided confidence interval, following a standard engineering statistics approach (NIST 2012)

$$\sigma_{\text{up}} = \sqrt{\frac{(n-1)s^2}{\chi^2_{n-1,\alpha}}}, \quad \sigma \leq \sigma_{\text{up}}, \tag{25}$$

where $\chi^2_{n-1,\alpha}$ is the χ^2-value that cuts an area equal to the significance level α of the Chi-squared distribution with $n-1$ degrees of freedom (Bortz 1999). For $n = 38$ and $\alpha = 5\%$, one obtains $\chi^2_{n-1,\alpha} = 24.1$; thus, Eq. (25) delivers $\sigma_{\text{up}} = 0.400$. Finally, we use the estimates for the characteristics of the normally distributed statistical population, namely the upper and lower bounds for the mean value μ_{up} and μ_{low} according to Eq. (24) as well as the upper bound for the standard deviation, σ_{up} according to Eq. (25), in order to obtain estimates for 5%- and the 95%-quantiles of the statistical population; i.e., we insert the aforementioned estimates in the standard definitions of quantiles, yielding

$$\log\left(\frac{d_{\text{pore},i}}{d^*_{\text{pore},i}}\right)_{5\%} = \mu_{\text{low}} - z_{0.025}\sigma_{\text{up}}, \tag{26}$$

$$\log\left(\frac{d_{\text{pore},i}}{d^*_{\text{pore},i}}\right)_{95\%} = \mu_{\text{up}} + z_{0.025}\sigma_{\text{up}}, \tag{27}$$

where $z_{\alpha/2}$ is the z-value that cuts an area equal to $(1-\alpha)$ of the standardized normal distribution. Evaluating Eqs. (26) and (27) for $\alpha = 5\%$, thus for $z_{0.025} = 1.645$, yields $\log(d_{\text{pore},i}/d^*_{\text{pore},i})_{5\%} = -23.427$ and $\log(d_{\text{pore},i}/d^*_{\text{pore},i})_{95\%} = -21.898$. Eventually, we can calculate the median of the $d_{\text{pore},i}$-population, $(d_{\text{pore}})_{50\%}$, its 5%-quantile, $(d_{\text{pore}})_{5\%}$, and its 95%-quantile, $(d_{\text{pore}})_{95\%}$:

$$\begin{aligned}
(d_{\text{pore}})_{50\%} &= 1.438 \times 10^{-10}\,\text{m}^2/\text{s},\\
(d_{\text{pore}})_{5\%} &= 6.698 \times 10^{-11}\,\text{m}^2/\text{s},\\
(d_{\text{pore}})_{95\%} &= 3.088 \times 10^{-10}\,\text{m}^2/\text{s}.
\end{aligned} \tag{28}$$

A graphical representation of these results, see Fig. 4, shows that all but one experimental data point are located within the bounds defined by the 5%-quantile and the 95%-quantile of the $d_{\text{pore},i}$-population. The respective outlier, however, is located within the bounds defined by the 2%-quantile and the 98%-quantile of the $d_{\text{pore},i}$-population, calculated analogously as

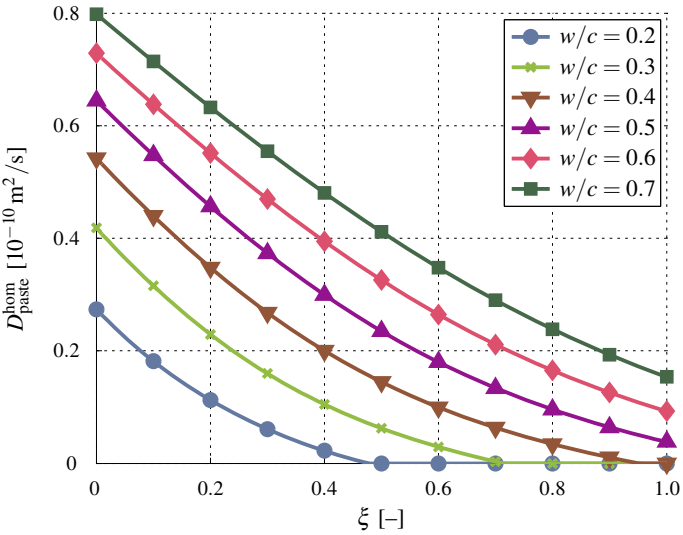

Fig. 5 $D^{\mathrm{hom}}_{\mathrm{paste}}$, as a function of the the hydration degree ξ, computed for different water-to-cement ratios

demonstrated above:

$$\begin{aligned}(d_{\mathrm{pore}})_{2\%} &= 5.391 \times 10^{-11}\,\mathrm{m}^2/\mathrm{s},\\ (d_{\mathrm{pore}})_{98\%} &= 3.837 \times 10^{-10}\,\mathrm{m}^2/\mathrm{s}.\end{aligned} \tag{29}$$

In addition to this satisfactory bounding characteristics, the trend predicted by the homogenization model of Sect. 3 fed with the median of the pore diffusivity, $(d_{\mathrm{pore}})_{50\%} = 1.438 \times 10^{-10}\,\mathrm{m}^2/\mathrm{s}$, describes the actual, experimentally given porosity–diffusivity trend remarkably well, as underlined by a coefficient of determination of $R^2 = 0.913$.

Finally, it is further instructive to assess the dependence of the macroscopic diffusivity of cement paste on the underlying cement paste mixture, quantified based on the initial water-to-cement ratio w/c, and on the hydration degree ξ. For this purpose, we evaluate Eq. (18) for various water-to-cement ratios ranging from 0.2 to 0.7, in order to get access to the mixture- and hydration degree-dependent pore space volume fraction $f_{\mathrm{pore}} = f_{\mathrm{water}}$. Equation (16) then allows us to study how the diffusivity of cement paste changes over its service life, for different cement paste mixtures, see Fig. 5.

5 Discussion

The herein presented homogenization approach starts at a local level where the physics is quite well understood, namely the diffusion of chloride ions in the pore space of cement paste, following Fick's law; we upscale this behavior to the level of cement paste where we again retrieve a Fick-type diffusion behavior. Such a mode of (physically reasonable) upscaling has been repeatedly described in the open literature, see, e.g., (Hashin 1968; Dormieux and Lemarchand 2001; Boutin and Geindreau 2010 and Patel et al. 2016). Thus, we would qualify our approach as a typical "micromechanics strategy." Concerning the "structural," "layered," or "glassy" water phase, it has been shown by the landmark molecular dynamics studies of Ichikawa et al. (2000, 2002) that the changes in physics due to the "structuring"

or "layering" of water molecules express themselves simply in a different, namely reduced, pore diffusivity, which, however, may still enter the upscaling strategy related to further above. From a more general viewpoint, we wish to remark that it is well known that the structure of water changes in the immediate vicinity of charged surfaces (such as the surfaces of hydrates), resulting in some kind of layering effect (Pollack 2001, 2013). Such kind of water domains are imagined to be glassy, or of ice-type ("liquid crystalline") nature, and are alternatively referred to as "surface zone" (Henniker 1949) or "exclusion zone" (Pollack 2013). Layered water exhibits physical properties that vary significantly from the properties of bulk water. For example, as shown by molecular dynamics studies, water layering leads to increased viscosity and reduced diffusivity (Ichikawa et al. 2000, 2002). The thickness of layered water can amount up to a few millimeters (Zheng et al. 2006, 2009b; Pollack 2013; Florea et al. 2014). This suggests that the pores pervading cement paste are entirely and homogeneously filled with layered water (instead of bulk water). In our model, this implies that the (chloride) diffusion coefficient of the pore fluid is, throughout the entire pore space, reduced with respect to the (chloride) diffusion coefficient in bulk water. At the same time, we are aware that there exist other propositions (Bertolini et al. 2004; Yang 2013) which limit the characteristic length scale of water molecule mobility restriction to several tens of nanometers; rather than to micrometers or even to millimeters. However, latest experiments and simulations on pore size distributions in concrete (Huang et al. 2015) reveal that typically 80% of the pore space found in very mature cement paste is made up by pores with characteristic lineal dimensions of less than 20 nanometers. This renders the aforementioned propositions (Bertolini et al. 2004; Yang 2013) as not necessarily at odds with our proposition of approximately homogeneous properties throughout the channel-like pore phases introduced in the herein-presented modeling approach. Furthermore, while we presently analyze, based on our "micromechanical" transport model, only *one* layered water diffusivity value allowing for the prediction of various diffusivity values at the cement paste level, we understand that this approach may be further refined in the future, by performing molecular dynamics studies targeting explicitly at the diffusivity determination of cement paste pore fluid. This is, however, beyond the scope of the present manuscript. We also wish to remark that our upscaling situation is different from that encountered when upscaling, by means of the asymptotic expansion technique, the Navier–Stokes equation to a permeability equation—then, the structure of the governing equations indeed changes upon scale transition, see, e.g., (Auriault and Lewandowska 1997; Auriault 2002; Boutin and Geindreau 2010).

The aforementioned molecular dynamics studies (Ichikawa et al. 2000, 2002) are particularly insightful, as they reveal that for a geomaterial which is somewhat similar to cement paste, i.e., clay, the diffusivity decreases from bulk to pore solution by a factor of 7; from $d_{\text{bulk}} = 1.61 \times 10^{-9}\,\text{m}^2/\text{s}$ to $d_{\text{pore}}^{\text{Ichikawa}} = 2.3 \times 10^{-10}\,\text{m}^2/\text{s}$. Our new prediction for the pore solution diffusivity, $\bar{d}_{\text{pore}} = 1.476 \times 10^{-10}\,\text{m}^2/\text{s}$ (being separated from the bulk solution diffusivity by factor 10.91) is considerably closer to molecular dynamics-derived pore solution diffusivity than the one reported in Sect. 1 of this paper, $d_{\text{pore}}^{\text{Pivonka}} = 1.07 \times 10^{-10}\,\text{m}^2/\text{s}$ (being separated from the bulk solution diffusivity by factor 15). In other words, the difference between micromechanics- and molecular dynamics-based pore solution diffusivity could be reduced by ≈32%. This confirms that the more realistic representation of cement paste according to Fig. 1 indeed leads to a more precise prediction of the cement paste diffusivity.

In view of the actual ordering of water molecules at the sub-nanometer scale of the "structured" or "layered" water phase, our concept involving an isotropic pore diffusivity may appear as bold approximation. Strictly speaking, the aforementioned molecular configuration would result in direction-dependent movement possibilities for the ions. In order to study the

implications of the isotropic pore diffusivity modeling followed so far, we now extend our analysis to a transversely isotropic pore diffusivity tensor reading as

$$\mathbf{d}_{\text{pore}}^{\text{aniso}} = \begin{bmatrix} d_{\text{pore}}^{\text{long}} & 0 & 0 \\ 0 & d_{\text{pore}}^{\text{trans}} & 0 \\ 0 & 0 & d_{\text{pore}}^{\text{trans}} \end{bmatrix}_{\mathbf{e}_r, \mathbf{e}_\vartheta, \mathbf{e}_\varphi}, \tag{30}$$

where $d_{\text{pore}}^{\text{long}}$ relates to the diffusivity in the pore direction and $d_{\text{pore}}^{\text{trans}}$ denotes the diffusivity orthogonal to it. Using this format for $\mathbf{d}_{\text{pore}}$ in the expression for the homogenized diffusivity tensor, i.e., Eq. (15), yields the following homogenized cement paste diffusivity:

$$D_{\text{paste}}^{\text{hom,aniso}} = \frac{1}{2(9+f_{\text{pore}})} \left\{ 2d_{\text{pore}}^{\text{long}} f_{\text{pore}} - 9d_{\text{pore}}^{\text{trans}} + 15d_{\text{pore}}^{\text{trans}} f_{\text{pore}} + \left[8d_{\text{pore}}^{\text{long}} d_{\text{pore}}^{\text{trans}} f_{\text{pore}}(9+f_{\text{pore}}) + \left(2d_{\text{pore}}^{\text{long}} f_{\text{pore}} + 3d_{\text{pore}}^{\text{trans}} (5f_{\text{pore}} - 3) \right)^2 \right]^{0.5} \right\}. \tag{31}$$

For the sake of demonstration, we have performed the back-calculation of the pore-scale diffusivity according to Eq. (31), by means of an evolution algorithm (Schwefel 1977), aiming at minimization of $1 - R^2$, R^2 being the coefficient of determination related to the deviation between the model predictions according to Eq. (31) and the experimental data according to Table 1. Such an optimization yields $d_{\text{pore}}^{\text{long}} = 1.470 \times 10^{-10}\,\text{m}^2/\text{s}$ and $d_{\text{pore}}^{\text{trans}} = 0.806 \times 10^{-10}\,\text{m}^2/\text{s}$, with the maximized coefficient of determination amounting to $R^2 = 0.9117$. It is now instructive to compare the performance of the model-predicted cement paste diffusivity based on anisotropic pore diffusivity behavior, to the one based on isotropic pore diffusivity behavior; for the latter, we evaluate Eq. (16), with $d_{\text{pore}} = 1.476 \times 10^{-10}\,\text{m}^2/\text{s}$, see Fig. 6. It turns out that the performances of the two modeling options are very similar. The most apparent difference is that an anisotropic pore-scale diffusivity consistently leads to lower homogenized diffusivities on the cement paste scale. However, this difference becomes relevant only for high-porosity cement pastes, i.e., for f_{pore} significantly larger than 0.3. Since only one experimental data point is available for $f_{\text{pore}} = 0.387$, and experimental data for cement paste porosities higher than that are not available to us, it appears that the true benefits of using an anisotropic pore-scale diffusivity tensor are yet to be unveiled. For the time being, we consider prescribing in our model an isotropic pore-scale diffusivity as reasonable model assumption because then the pore-scale diffusion coefficient can be simply back-calculated from the experimental data, not requiring the use of a more expensive optimization algorithm.

We may also mention that our approach is fully consistent with the current state of the art in the mathematical modeling of concrete: In fact, our microheterogeneous formulation rests on the famous hydration model of Powers and Brownyard (1948) and Acker (2001), which has not only provided the basis for numerous, experimentally validated, micromechanical descriptions (Hellmich and Mang 2005; Sanahuja et al. 2007; Pichler et al. 2009b; Scheiner and Hellmich 2009), but has also been kind of corroborated by very recent statistical physics approaches (Ioannidou et al. 2016). In the aforementioned micromechanics approaches, an RVE of cement paste is either composed of water pores, air pores, hydrates, and unhydrated cement (clinker) grains (Hellmich and Mang 2005; Pichler et al. 2009b; Scheiner and Hellmich 2009), or of clinker grains embedded into a hydrate foam matrix, whereby the latter is, at a smaller scale, resolved into hydrates, water pores, and air pores; i.e., a hierarchical system of two RVEs is used to represent cement paste (Pichler and Hellmich 2011; Pichler

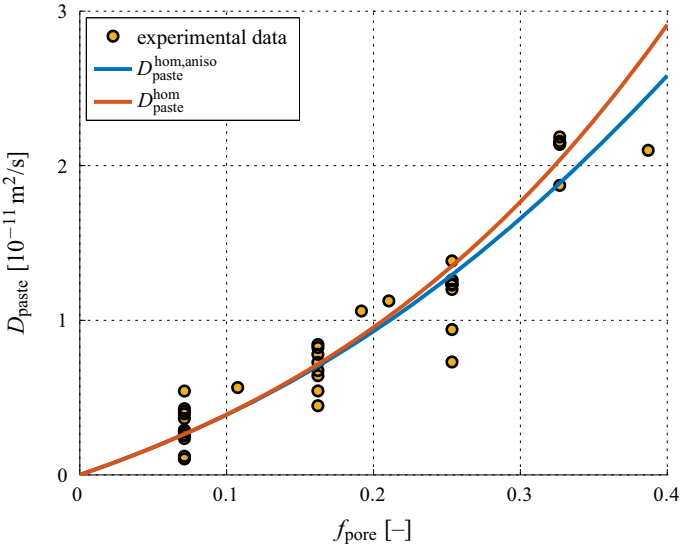

Fig. 6 Comparison of D_{paste}^{exp} according to the experimental studies listed in Table 1, $D_{paste}^{hom,aniso}$ for anisotropic pore diffusivity, according to Eq. (31), with $d_{pore}^{long} = 1.470 \times 10^{-10}$ m^2/s and $d_{pore}^{trans} = 0.806 \times 10^{-10}$ m^2/s, and D_{paste}^{hom} for isotropic pore diffusivity, according to Eq. (16), with $d_{pore} = 1.476 \times 10^{-10}$ m^2/s

et al. 2013). Presently, our transport modeling approach somewhat follows the material phase description of Hellmich and Mang (2005), Pichler et al. (2009b) and Scheiner and Hellmich (2009), involving only one RVE representing the composite material cement paste. Actually, we additionally merge, on the one hand, the water and air pore phases into one phase called "capillary porosity" (this merging results from the experimental conditions realized in standard diffusion tests), and on the other hand, the hydrate and clinker phases are merged as well, into one "solid phase" (given their non-diffusible nature as compared to that of the pores). This concept, involving only one RVE, seems to be particularly well suited for the present situation where we restrict our investigations to fully hydrated cement pastes. In this case, no unhydrated cement clinker is left, and even the aforementioned two-scale formulations degenerate into a one-scale formulation. Still, it is interesting to find out up to which extent our homogenization scheme improves similar earlier developments, such as the differential homogenization scheme of Dormieux and Lemarchand (2001), which has been applied to cement paste diffusivity by Pivonka et al. (2004), and the "self-consistent bispherical model" of Hashin (1968). An analysis as described in Sect. 3 was performed for both alternative homogenization schemes. While the homogenization approach presented in Sect. 4 yields a pore-scale chloride diffusivity separated from the chloride diffusivity in bulk solution by factor 10.91, the homogenization schemes of Dormieux and Lemarchand (2001) and Hashin (1968), respectively, yield pore-scale chloride diffusivities separated from the chloride diffusivity in bulk solution by factors 13.16 and 24.16, respectively. Considering that the molecular dynamics studies of Ichikawa et al. (2000, 2002) suggest that this factor amounts to 7, we conclude that our model yields significantly more accurate results than previous models. All these homogenization approaches may be qualified as "Fickian diffusion," delivering diffusivity quantities which relate concentration gradients to molar fluxes. Limitations of such approaches have been extensively discussed, and it is of interest to review these limitations in the context of our work: Non-Fickian diffusion induces significant, non-negligible deforma-

tions in the respective porous material, because of which the mathematical description of the diffusion process needs to be extended (as compared to the classical Fick's law), in order to take into account the interaction between deformation-induced stresses and Brownian motion (Ferreira et al. 2015). This is, however, not the case in the problem studied here. Another limitation of the Fickian description related to heterogeneity is: The homogenized diffusivity needs to be defined on an RVE already fulfilling the separation of scales requirement between micro-heterogeneity and RVE size, on the one hand, and between RVE size and size of the structural geometry or loading, on the other hand. In cases where this requirement is violated (Neuman and Tartakovsky 2009; Fourar and Radilla 2009), non-Fickian descriptions are needed.

From the viewpoint of classical self-consistent modeling (Hershey 1954; Hill 1965), it may seem surprising that our approach does not exhibit a percolation threshold, i.e., a minimum porosity needed to allow for ionic transport. This owes to the elongated shape of the cylindrical pores, ensuring a connected, and thus diffusion-enabling network even for arbitrarily small porosities. This changes if the pore space is considered to be of non-cylindrical shape. For example, evaluating our homogenization scheme for spherical pores yields a cement paste diffusivity of

$$D_{\text{paste}}^{\text{hom,sph}} = \begin{cases} \dfrac{d_{\text{pore}}}{2}\left(3f_{\text{pore}} - 1\right) & \text{for } f_{\text{pore}} \geq \frac{1}{3} \\ 0 & \text{for } f_{\text{pore}} < \frac{1}{3}, \end{cases} \tag{32}$$

indicating a percolation threshold of $f_{\text{pore}} = \frac{1}{3}$, below which no ionic transport is possible. As discussed in (Pichler et al. 2009a), cylindrical pores imply the lower bound for the diffusivity-related percolation threshold of cement paste, while spherical pores imply the respective upper bound, see also Fig. 7 for a graphical comparison of $D_{\text{paste}}^{\text{hom}}$ according to Eq. (16) and $D_{\text{paste}}^{\text{hom,sph}}$ as defined above; prescribing oblate or prolate spheroids (with finite aspect ratios) as pore shapes would imply percolation thresholds somewhere between $0 \leq f_{\text{pore}} \leq \frac{1}{3}$. In the present case, we focus on fully hydrated cement paste, with $f_{\text{pore}} \geq 0.071$. As demonstrated in experimental studies, see Table 1, such cement paste porosities *always* imply a connected network of capillary pores enabling diffusive transport of species dissolved in the pore solution. Thus, for the consideration of cement paste diffusivities, any percolation thresholds *not* being close to $f_{\text{pore}} = 0$ make very limited sense.

It is also interesting to discriminate our approach from the popular "effective medium approaches." The latter go back to the seminal work of Maxwell Garnett (Garnett 1904) and have been adapted to diffusivity upscaling by Burganos and Sotirchos (1987). However, quoting from (Levy and Stroud 1997), effective medium approaches are *"useful when one of the components can be considered as a host in which inclusions of the other components are embedded."* This implies that the effective medium theory is probably not useful for estimating the diffusivity of cement paste, at least not when considering the morphology according to Fig. 1. In contrast, the effective medium theory is indeed useful for estimation of concrete, see, e.g., (Oh and Jang 2004), which is, however, beyond the scope of this paper.

6 Summary and Outlook

Recent developments in continuum homogenization theories extended to infinitely many material phases related to all orientations in Euclidean space (Fritsch et al. 2009, 2013; Abdalrahman et al. 2015) could be successfully applied to diffusivity upscaling. The corresponding results allow for improved representation of water-to-cement ratio-dependent and

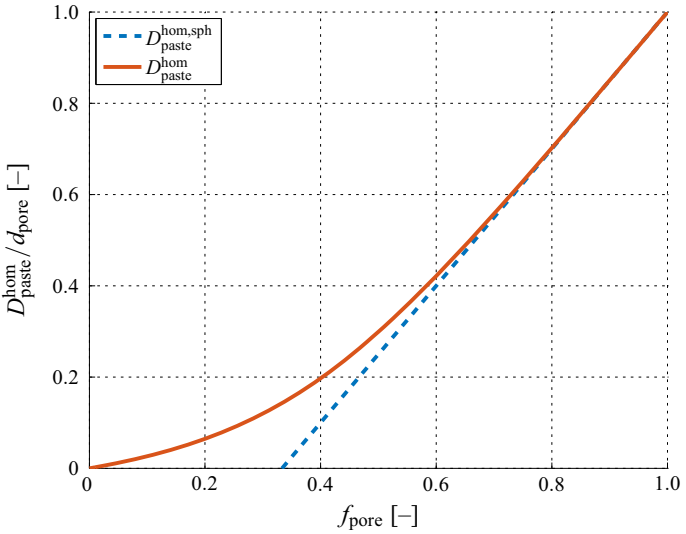

Fig. 7 Comparison of $D_{\text{paste}}^{\text{hom}}$ according to Eq. (13) of the revised paper, considering cylindrically shaped pores, to $D_{\text{paste}}^{\text{hom,sph}}$ according to Eq. (32), considering spherically shaped pores; the former does not exhibit any percolation threshold, while the latter features percolation at $f_{\text{pore}} = \frac{1}{3}$

hydration-dependent diffusivity of cement paste. This provides a novel, both experimentally and theoretically improved foundation which may support large-scale simulations concerning durability of concrete structures, see, e.g., the approaches presented by Schrefler and Pesavento (2004), Gawin et al. (2006).

Future model developments may include extension of the homogenization scheme from the cement paste to the concrete level. For this purpose, additional interface phenomena, possibly occurring between the cement matrix and the aggregate grains (van Breugel et al. 2004) may deserve particular attention. Another interesting extension of the present model could relate to the case of unsaturated pores. This could be done based on the very interesting recent suggestion (Yang et al. 2016) of covering an Eshelby inclusion representing the solid phase by a liquid layer. This extension should be readily applicable to the Eshelby problem of Fig. 1b; together with the introduction of a new Eshelby problem related to the empty pore spaces, i.e., to a gaseous phase.

Acknowledgements Open access funding provided by TU Wien (TUW). Financial support by the Austrian Federal Ministry of Science and Research (BMWF), in the frame of the ASEA UNINET-Program, and by the Thailand Research Fund (TRF), via Grant MRG5580222, is gratefully acknowledged.

References

Abdalrahman, T., Scheiner, S., Hellmich, C.: Is trabecular bone permeability governed by molecular ordering-induced fluid viscosity gain? Arguments from re-evaluation of experimental data in the framework of homogenization theory. J. Theor. Biol. **365**, 433–444 (2015)

Acker, P.: Micromechanical analysis of creep and shrinkage mechanisms. In: Ulm, F.-J., Bažant, Z., Wittmann, F. (eds.) Concreep 6: Creep, Shrinkage and Durability of Concrete and Concrete Structures, Cambridge, pp. 15–25. Elsevier, Amsterdam (2001)

Auriault, J.-L.: Upscaling heterogeneous media by asymptotic expansions. J. Eng. Mech. (ASCE) **128**(8), 817–822 (2002)

Auriault, J.-L., Lewandowska, J.: Effective diffusion coefficient: from homogenization to experiment. Transp. Porous Media **27**(2), 205–223 (1997)

Bertolini, L., Elsener, B., Pedeferri, P., Polder, R.: Corrosion of Steel in Concrete. Wiley-VCH GmbH & Co, Weilheim (2004)

Bortz, J.: Statistik für Sozialwissenschaftler [Statistics for social scientists]. Springer, Berlin (1999). (**In German**)

Boutin, C., Geindreau, C.: Periodic homogenization and consistent estimates of transport parameters through sphere and polyhedron packings in the whole porosity range. Phys. Rev. B **82**, 036313 (2010)

Burganos, V., Sotirchos, S.: Diffusion in pore networks: effective medium theory and smooth field approximation. AIChE J. **33**(10), 1678–1689 (1987)

Caré, S.: Influence of aggregates on chloride diffusion coefficient into mortar. Cem. Concr. Res. **33**(7), 1021–1038 (2003)

Castellote, M., Alonso, C., Andrade, C., Chadbourn, G., Page, C.: Oxygen and chloride diffusion in cement pastes as a validation of chloride diffusion coefficients obtained by steady-state migration tests. Cem. Concr. Res. **31**(4), 621–625 (2001)

Dormieux, L., Kondo, D.: Approche micromécanique du couplage perméabilité—endommagement [Micromechanical approach to the approach to the coupling between permeability and damage]. Comptes Rendus Mécanique **332**(2), 135–140 (2004). (**In French**)

Dormieux, L., Kondo, D.: Applied Micromechanics of Porous Media, volume 480 of CISM Courses and Lecture Series, Lecture Notes Chapter 2—Diffusive Transport in Disordered Media. Application to the Determination of the Tortuosity and the Permeability of Cracked Materials, pp. 83–106. Springer, Wien (2005)

Dormieux, L., Kondo, D., Ulm, F.-J.: Microporomechanics. Wiley, New York (2006)

Dormieux, L., Lemarchand, E.: Homogenization approach of advection and diffusion in cracked porous material. J. Eng. Mech. **127**(12), 1267–1274 (2001)

Drugan, W., Willis, J.: A micromechanics-based nonlocal constitutive equation and estimates of representative volume element size for elastic composites. J. Mech. Phys. Solids **44**(4), 497–524 (1996)

Du, X., Jin, L., Ma, G.: A meso-scale numerical method for the simulation of chloride diffusivity in concrete. Finite Elem. Anal. Des. **85**, 87–100 (2014)

Eshelby, J.: The determination of the elastic field of an ellipsoidal inclusion, and related problems. Proc. R Soc. Lond. Ser. A **241**, 376–396 (1957)

Ferreira, J., Grassi, M., Gudiño, E., de Oliveira, P.: A new look to non-Fickian diffusion. Appl. Math. Model. **39**(1), 194–204 (2015)

Florea, D., Musa, S., Huyghe, J., Wyss, H.: Long-range repulsion of colloids driven by ion exchange and diffusiophoresis. Proc. Natl. Acad. Sci. USA **111**(18), 6554–6559 (2014)

Fourar, M., Radilla, G.: Non-Fickian description of tracer transport through heterogeneous porous media. Transp. Porous Media **80**(3), 561–579 (2009)

Fritsch, A., Dormieux, L., Hellmich, C., Sanahuja, J.: Mechanical behavior of hydroxyapatite biomaterials: an experimentally validated micromechanical model for elasticity and strength. J. Biomed. Mater. Res. Part A **88A**(1), 149–161 (2009)

Fritsch, A., Hellmich, C., Young, P.: Micromechanics-derived scaling relations for poroelasticity and strength of brittle porous polycrystals. J. Appl. Mech. (ASME) **80**(2), 020905 (2013)

Garnett, J.: Colours in metal glasses and in metallic films. Philos. Trans. R. Soc. Lond. A **203**(359–371), 385–420 (1904)

Gawin, D., Pesavento, F., Schrefler, B.: Hygro-thermo-chemo-mechanical modelling of concrete at early ages and beyond. Part I: hydration and hygro-thermal phenomena. Int. J. Numer. Methods Eng. **67**(3), 299–331 (2006)

Germain, P.: The method of virtual power in continuum mechanics. Part 2: microstructure. SIAM J. Appl. Math. Appl. Math. **25**(3), 556–575 (1973)

Glass, G., Buenfeld, N.: The presentation of the chloride threshold level for corrosion of steel in concrete. Corros. Sci. **39**(5), 1001–1013 (1997)

Glasser, F., Marchand, J., Samson, E.: Durability of concrete—degradation phenomena involving detrimental chemical reactions. Cem. Concr. Res. **38**(2), 226–246 (2008)

Hashin, Z.: Assessment of the self-consistent approximation: conductivity of particulate composites. J. Compos. Mater. **2**(3), 284–300 (1968)

Hellmich, C., Mang, H.: Shotcrete elasticity revisited in the framework of continuum micromechanics: from submicron to meter level. J. Mater. Civ. Eng. (ASCE) **17**(3), 246–256 (2005)
Henniker, J.: The depth of the surface zone of a liquid. Rev. Mod. Phys. **21**, 322–341 (1949)
Hershey, A.: The elasticity of an isotropic aggregate of anisotropic cubic crystals. ASME J. Appl. Mech. **21**, 236–240 (1954)
Hill, R.: A self-consistent mechanics of composite materials. J. Mech. Phys. Solids **13**(4), 213–222 (1965)
Hornain, H., Marchand, J., Duhot, V., Moranville-Regourd, M.: Diffusion of chloride ions in limestone filler blended cement pastes and mortars. Cem. Concr. Res. **25**(8), 1667–1678 (1995)
Huang, Q., Jiang, Z., Gu, X., Zhang, W., Guo, B.: Numerical simulation of moisture transport in concrete based on a pore size distribution model. Cem. Concr. Res. **67**, 31–43 (2015)
Huang, X.-F., Zheng, J.-J., Zhou, X.-Z.: Simple analytical solution for the chloride diffusivity of cement paste. Sci. Technol. Overseas Build. Mater. **32**(2), 4–6 (2010)
Ichikawa, Y., Kawamura, K., Fujii, N., Nattavut, T.: Molecular dynamics and multiscale homogenization analysis of seepage/diffusion problem in bentonite clay. Int. J. Numer. Methods Eng. **54**(12), 1717–1749 (2002)
Ichikawa, Y., Kawamura, K., Nakano, M., Kitayama, K., Fujii, N.: Molecular behavior and micro/macro analysis of diffusion problem in bentonite. In: CD-ROM Proceedings of the European Congress on Computational Methods in Applied Sciences and Engineering, Barcelona (2000)
Ioannidou, K., Krakowiak, K., Bauchy, M., Hoover, C., Masoero, E., Yip, S., Ulm, F.-J., Levitz, P., Pellenq, R.J.-M., Del Gado, E.: Mesoscale texture of cement hydrates. Proc. Natl. Acad. Sci. USA **113**(8), 2029–2034 (2016)
König, G., Soukhov, D., Jungwirth, F.: Betondruckfestigkeit nach prEN 206 und EC 1/EC 2 - Sichere Betonproduktion [Compressive strength of concrete according to prEN 206 and EC 1/EC 2 - safe production of concrete]. Beton (11), 680 (1998). (**In German**)
Kuhl, D., Bangert, F., Meschke, G.: Coupled chemo-mechanical deterioration of cementitious materials part II: numerical methods and simulations. Int. J. Solids Struct. **41**(1), 41–67 (2004)
Levy, O., Stroud, D.: Maxwell Garnett theory for mixtures of anisotropic inclusions: application to conducting polymers. Phys. Rev. B **56**(13), 8035–8046 (1997)
Liu, L., Chen, H., Sun, W., Ye, G.: Microstructure-based modeling of the diffusivity of cement paste with micro-cracks. Constr. Build. Mater. **38**, 1107–1116 (2013)
Liu, L., Sun, W., Ye, G., Chen, H., Qian, Z.: Estimation of the ionic diffusivity of virtual cement paste by random walk algorithm. Constr. Build. Mater. **28**(1), 405–413 (2012)
Lutz, M., Zimmerman, R.: Effect of the interface zone on the conductivity or diffusivity of a particulate composite using Maxwell's homogenization method. Int. J. Eng. Sci. **98**, 51–59 (2015)
MacDonald, K., Northwood, D.: Experimental measurements of chloride ion diffusion rates using a two-compartment diffusion cell: effects of materials and test variables. Cem. Concr. Res. **25**(7), 1407–1416 (1995)
Maugin, G.: The principle of virtual power: from eliminating metaphysical forces to providing an efficient modelling tool. Contin. Mech. Thermodyn. **25**(2), 127–146 (2013)
Meille, S., Garboczi, E.: Linear elastic properties of 2D and 3D models of porous materials made from elongated objects. Model. Simul. Mater. Sci. Eng. **9**(5), 371–390 (2001)
Neuman, S., Tartakovsky, D.: Perspective on theories of non-Fickian transport in heterogeneous media. Adv. Water Resour. **32**(5), 670–680 (2009)
Ngala, V., Page, C.: Effects of carbonation on pore structure and diffusional properties of hydrated cement pastes. Cem. Concr. Res. **27**(7), 995–1007 (1997)
Ngala, V., Page, C., Parrott, L., Yu, S.: Diffusion in cementitious materials: 2. Further investigations of chloride and oxygen diffusion in well-cured OPC and OPC/20% PFA pastes. Cem. Concr. Res. **25**(4), 819–826 (1995)
NIST: NIST/SEMATECH e-Handbook of Statistical Methods. National Institute of Standards and Technology (2012)
Oh, B., Jang, S.: Prediction of diffusivity of concrete based on simple analytic equations. Cem. Concr. Res. **34**(3), 463–480 (2004)
Page, C., Ngala, V.: Steady-state diffusion characteristics of cementitious materials. In: Nilson, L.-O., Ollivier, J. (eds.) Proceedings of the RILEM International Workshop on 'Chloride Penetration Into Concrete', pp. 77–84. RILEM Publishing, Cachan (1997)
Page, C., Short, N., Tarras, A.: Diffusion of chloride ions in hardened cement pastes. Cem. Concr. Res. **11**(3), 395–406 (1981)
Patel, R., Phung, Q., Seetharam, S., Perko, J., Jacques, D., Maes, N., De Schutter, G., Ye, G., van Breugel, K.: Diffusivity of saturated ordinary Portland cement-based materials: a critical review of experimental and analytical modelling approaches. Cem. Concr. Res. **90**, 52–72 (2016)

Pichler, B., Hellmich, C.: Upscaling quasi-brittle strength of cement paste and mortar: a multi-scale engineering mechanics model. Cem. Concr. Res. **41**(5), 467–476 (2011)
Pichler, B., Hellmich, C., Eberhardsteiner, J.: Spherical and acicular representation of hydrates in a micromechanical model for cement paste: prediction of early-age elasticity and strength. Acta Mech. **203**(3–4), 137–162 (2009a)
Pichler, B., Hellmich, C., Eberhardsteiner, J., Wasserbauer, J., Termkhajornkit, P., Barbarulob, R., Chanvillard, G.: Effect of gel–space ratio and microstructure on strength of hydrating cementitious materials: an engineering micromechanics approach. Cem. Concr. Res. **45**, 55–68 (2013)
Pichler, B., Hellmich, C., Mang, H.: Impact of rocks onto gravel—design and evaluation of experiments. Int. J. Impact Eng. **31**(5), 559–578 (2005)
Pichler, B., Scheiner, S., Hellmich, C.: From micron-sized needle-shaped hydrates to meter-sized shotcrete tunnel shells: micromechanical upscaling of stiffness and strength of hydrating shotcrete. Acta Geotech. **3**(4), 273–294 (2009b)
Pivonka, P., Hellmich, C., Smith, D.: Microscopic effects on chloride diffusivity of cement pastes—a scale-transition analysis. Cem. Concr. Res. **34**(12), 2251–2260 (2004)
Pollack, G.: Cells, Gels, Engines of Life. Ebner and Sons, Seattle (2001)
Pollack, G.: The Fourth Phase of Water Beyond Solid, Liquid, and Vapor. Ebner and Sons, Seattle (2013)
Powers, T., Brownyard, T.: Studies of the physical properties of hardened Portland cement paste. Res. Lab. Portland Cem. Assoc. Bull. **22**, 101–992 (1948)
Robinson, R., Stokes, R.: Electrolyte Solution, 2nd edn. Butterworths, London (1959)
Salençon, J.: Handbook of Continuum Mechanics. Springer, Berlin (2001)
Sanahuja, J., Dormieux, L., Chanvillard, G.: Modelling elasticity of a hydrating cement paste. Cem. Concr. Res. **37**(10), 1427–1439 (2007)
Sanahuja, J., Dormieux, L., Meille, S., Hellmich, C., Fritsch, A.: Micromechanical explanation of elasticity and strength of gypsum: from elongated anisotropic crystals to isotropic porous polycrystals. J. Eng. Mech. (ASCE) **136**(2), 239–253 (2010)
Scheiner, S., Hellmich, C.: Continuum microviscoelasticity model for aging basic creep of early-age concrete. J. Eng. Mech. (ASCE) **135**(4), 307–323 (2009)
Schrefler, B., Pesavento, F.: Multiphase flow in deforming porous material. Comput. Geotech. **31**(3), 237–250 (2004)
Schwefel, H.-P.: Numerische Optimierung von Computer-Modellen mittels der Evolutionsstrategie [Numerical Optimization of Computer Models by means of the Evolution Strategy]. Birkhäuser Verlag, Basel und Stuttgart (1977). (**In German**)
Stewart, M., Rosowsky, D.: Structural safety and serviceability of concrete bridges subject to corrosion. J. Infrastruct. Syst. **4**(4), 146–155 (1998)
Student, : The probable error of a mean. Biometrika **6**(1), 1–25 (1908)
Sun, G., Zhang, Y., Sun, W., Liu, Z., Wang, C.: Multi-scale prediction of the effective chloride diffusion coefficient of concrete. Constr. Build. Mater. **25**(10), 3820–3831 (2011a)
Sun, G.-W., Sun, W., Zhang, Y.-S., Liu, Z.-Y.: Relationship between chloride diffusivity and pore structure of hardened cement paste. J. Zheijang Univ. Sci. A **12**(5), 360–367 (2011b)
Suquet, P.: Continuum Micromechanics, volume 377 of CISM Courses and Lectures. Springer, Wien (1997)
Tang, L., Nilson, L.-O.: Rapid determination of chloride diffusivity in concrete by applying an electric field. ACI Mater. J. **89**(1), 49–53 (1992)
van Breugel, K., Koenders, E., Guang, Y., Lura, P.: Modelling of transport phenomena at cement matrix-aggregate interface. Interface Sci. **12**(4), 423–431 (2004)
Wong, H., Pappas, A., Zimmerman, R., Buenfeld, N.: Effect of entrained air voids on the microstructure and mass transport properties of concrete. Cem. Concr. Res. **41**(10), 1067–1077 (2011)
Wong, H., Zobel, M., Buenfeld, N., Zimmerman, R.: Influence of the interfacial transition zone and microcracking on the diffusivity, permeability and sorptivity of cement-based materials after drying. Mag. Concr. Res. **61**(8), 571–589 (2009)
Wu, Z., Wong, H., Buenfeld, N.: Influence of drying-induced microcracking and related size effects on mass transport properties of concrete. Cem. Concr. Res. **68**, 35–48 (2015)
Yang, R.: Contributions to Micromechanical Modelling of Transport and Freezing Phenomena within Unsaturated Porous Media. PhD Thesis, Université Paris-Est (2013)
Yang, R., Lemarchand, E., Fen-Chong, T.: A micromechanics model for solute diffusion coefficient in unsaturated granular materials. Transp. Porous Media **111**(2), 347–368 (2016)
Yu, S., Page, C.: Diffusion in cementitious materials: 1. Comparative study of chloride and oxygen diffusion in hydrated cement pastes. Cem. Concr. Res. **21**(4), 581–588 (1991)
Zaoui, A.: Structural Morphology and Constitutive Behavior of Microheterogeneous Materials, Chapter 6, pp. 291–347. Springer, Wien (1997)

Zaoui, A.: Continuum micromechanics: survey. J. Eng. Mech. (ASCE) **128**(8), 808–816 (2002)
Zheng, J., Zhou, X.: Analytical solution for the chloride diffusivity of hardened cement paste. J. Mater. Civ. Eng. (ASCE) **20**(5), 384–391 (2008)
Zheng, J., Zhou, X., Wu, M.: A simple method for predicting the chloride diffusivity of cement paste. Mater. Struct. **43**(1), 99–106 (2010)
Zheng, J.-J., Wong, H., Buenfeld, N.: Assessing the influence of ITZ on the steady-state chloride diffusivity of concrete using a numerical model. Cem. Concr. Res. **39**(9), 805–813 (2009a)
Zheng, J.-M., Chin, W.-C., Khijniak, E., Khijniak Jr., E., Pollack, G.: Surfaces and interfacial water: evidence that hydrophilic surfaces have long-range impact. Adv. Colloid Interface Sci. **127**(1), 19–27 (2006)
Zheng, J.-M., Wexler, A., Pollack, G.: Effect of buffers on aqueous solute-exclusion zones around ion-exchange resins. J. Colloid Interface Sci. **332**(2), 511–514 (2009b)
Zienkiewicz, O., Taylor, R., Zhu, J.: The Finite Element Method: Its Basis and Fundamentals, 6th edn. Butterworth Heinemann, Oxford (2005)